Journal of Hazardous Materials 469 (2024) 133874

Contents lists available at ScienceDirect

Journal of Hazardous Materials

journal homepage: www.elsevier.com/locate/jhazmat

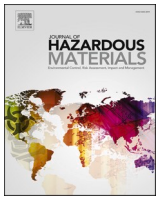

Classification of asbestos and their nonasbestiform analogues using FTIR and multivariate data analysis

Taekhee Lee *, Steven E. Mischler, Cody Wolfe

Health Hazards Prevention Branch, Pittsburgh Mining Research Division, National Institute for Occupational Safety and Health, Centers for Disease Control and Prevention, Pittsburgh, PA 15236, USA

HIGHLIGHTS

- Asbestos and analogues were classified using FTIR and multivariate data analysis.
- Classification of asbestos types with the method is possible.
- Classification of asbestos and their non-asbestiform analogues is also possible.
- PLS-DA of KBr pellet samples has an average 0.7% chance of misclassification.
- PLS-DA of PVC filter samples has an average 4.6% chance of misclassification.

GRAPHICAL ABSTRACT

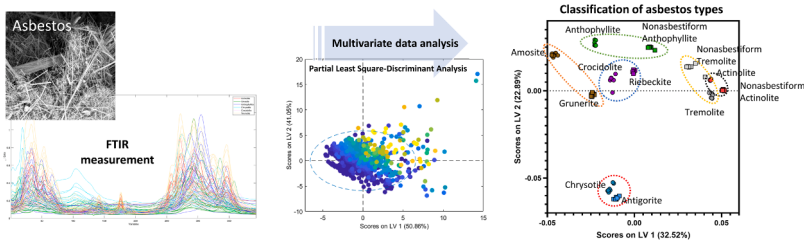

ARTICLE INFO

Keywords:
Asbestos classification
FTIR
Principal component analysis
Partial least squares-discriminant analysis

ABSTRACT

This study presents a possible application of Fourier transform infrared (FTIR) spectrometry and multivariate data analysis, principal component analysis (PCA), and partial least squares-discriminant analysis (PLS-DA) for classifying asbestos and their nonasbestiform analogues. The objectives of the study are: 1) to classify six regulated asbestos types and 2) to classify between asbestos types and their nonasbestiform analogues. The respirable fraction of six regulated asbestos types and their nonasbestiform analogues were prepared in potassium bromide pellets and collected on polyvinyl chloride membrane filters for FTIR measurement. Both PCA and PLS-DA classified asbestos types and their nonasbestiform analogues on the score plots showed a very distinct clustering of samples between the serpentine (chrysotile) and amphibole groups. The PLS-DA model provided ~95% correct prediction with a single asbestos type in the sample, although it did not provide all correct predictions for all the challenge samples due to their inherent complexity and the limited sample number. Further studies are necessary for a better prediction level in real samples and standardization of sampling and analysis procedures.

1. Introduction

The exposures to airborne asbestos fibers and other elongate mineral particles (EMPs) in occupational and natural environments can cause asbestosis, pulmonary inflammation, mesothelioma, and other cancers [9,17,18,29,31]. The number of deaths due to work-related asbestosis and malignant mesothelioma during 2005–2014 in the U.S. were 13,024 and 27,284, respectively [44]. Asbestos causes an estimated 255,000

* Correspondence to: Health Hazards Prevention Branch, Pittsburgh Mining Research Division, National Institute for Occupational Safety and Health, 626 Cochrans Mill Road, Pittsburgh, PA 15236, USA.
E-mail address: fwc8@cdc.gov (T. Lee).

https://doi.org/10.1016/j.jhazmat.2024.133874
Received 11 October 2023; Received in revised form 8 February 2024; Accepted 22 February 2024
Available online 24 February 2024
0304-3894/Published by Elsevier B.V.

deaths annually, and work-related exposures are responsible for 233,000 deaths worldwide [11]. Many countries are still producing asbestos (Collegium [8]), and asbestos-containing products are available in the U.S. market [27]. There are many analytical techniques available to characterize asbestos and other EMPs including phase contrast microscopy (PCM), polarized light microscopy (PLM), scanning electron microscopy (SEM), transmission electron microscopy (TEM), vibrational spectroscopies (Fourier Transform Infrared (FTIR) and Raman), and X-ray diffraction (XRD). The recommended analytic techniques are dependent on the sample matrix [15], and the combination of the analysis is a reasonable approach. For example, PCM is recommended for airborne asbestos and other fibers exposure index, and TEM is recommended for asbestos identification [39]. Although previous literature has shown the advantages of using IR for the measurement of asbestos (fast-within minutes of sample measurement, non-destructive, sensitive, and cost-effective) [3,12,46], the analysis method has not gained wide acceptance due to its limitations [20]. The limitations of asbestos analysis with traditional IR include: 1) difficulty distinguishing asbestos from their nonasbestiform analogues which are the same minerals (identical chemical and atomic structure) but with different growth habits and 2) inaccuracy of quantification due to the presence of confounding minerals in the samples. The National Institute for Occupational Safety and Health (NIOSH) has a continuing project to create a direct-on-filter measurement method for respirable crystalline silica (RCS) using portable FTIR spectrometers for field-based measurement including generating results at the end of the shift [6,7,16,33,34], which provides rapid exposure levels compared to the laboratory analytic methods. Multivariate data analysis has been applied on the FTIR spectra to reduce uncertainties due to confounding minerals with the possible benefit of more accurate prediction of RCS exposure levels when dealing with samples with complex mineralogy [35,48,50,51,54,55] and assist interpretation and classification of information-rich spectra [53]. In addition, the application of FTIR and multivariate analysis has been shown to accurately identify pigments and temperas on historical paintings [45], mineralogical composition of ancient pottery [32], mineral components of shale rocks [38] and to distinguish biological samples including COVID-19 infections and diseased cells [2,37,53]. The measurement technique with FTIR and multivariate data analysis hasn't been applied on asbestos identification, and if it is achievable, the analysis could be an alternative asbestos analytical technique. This study is the first attempt in using FTIR and multivariate data analysis, including principal component analysis (PCA) and partial least squares-discriminant analysis (PLS-DA) to: 1) classify the six regulated asbestos minerals–actinolite, amosite, anthophyllite, chrysotile, crocidolite, and tremolite and 2) classify between asbestos minerals and their nonasbestiform analogues–actinolite, grunerite, anthophyllite, antigorite, riebeckite, and tremolite.

2. METHOD AND MATERIALS

2.1. Asbestos and their analogues

The following well-characterized asbestos minerals and their analogues were used in this study (Table 1, Regulated asbestos): 1) actinolite (National Institute for Standard and Technology (NIST) standard reference materials (SRM), NIST SRM 1867), 2) amosite (NIST SRM 1866), 3) anthophyllite (Palm Springs, CA), 4) chrysotile (NIST SRM 1866), 5) crocidolite (NIST SRM 1866), and 6) tremolite (Lone Pine, CA). Asbestos nonasbestiform analogues include: 1) actinolite (San Bernadino Co., CA), 2) grunerite (Marquette Co., MI), 3) anthophyllite (Kopparberg, Sweden), 4) antigorite (Estrie, Quebec, Canada), 5) riebeckite (Pike's Peak, CO), 6) tremolite cleavage fragment (National Institute of Environmental Health Sciences (NIEHS), prepared by the U. S. Bureau of Mines). Most of the materials were fully characterized and utilized in previous studies [13,14,19].

2.2. Potassium bromide pellet samples and FTIR measurement

To collect a respirable-size fraction of asbestos and their nonasbestiform analogues, each mineral was placed in a Pyrex tube with 100-μm copper beads (TSI Inc., Shoreview, MN, USA) that was fixed on a vortex mixer (Vortex-Genie 2, Scientific Industries Inc.) and generated using a vortex mixer shaking method [21,22,24]. During vortex mixing, filtered air entered the Pyrex tube through a port at the top of the tube enabling aerosol suspension. The respirable-size fraction of the particles was then collected using GK4.126 cyclones loaded with polycarbonate filters (47-mm, pore size 1.0 μm, operating at 9.0 liter/min) [26]. The collected samples were scraped off the filters to prepare potassium bromide (KBr) pellet samples. The mass of each respirable-size fraction of the samples was weighed using a microbalance and mixed with 150 mg of KBr. Mixed samples were pressed using a 13-mm KBr pellet die (Specac Ltd, Orpington, UK) and a hydraulic pellet press (MSE Supplies, Tucson, AZ, USA). Each KBr pellet was analyzed with a portable FTIR (Alpha, Bruker, Billerica, MA) using the saved file of the blank KBr as a background, and spectra were collected in transmission mode at 4 cm^{-1} resolution by averaging 32 scans. FTIR measurement duration for each sample was less than a minute.

2.3. Air sampling and FTIR measurement

Polyvinyl chloride (PVC, 25-mm, pore size 5.0 μm, SKC Inc., Eighty Four, PA USA) and mixed cellulose ester (MCE, 25-mm, pore size 0.8 μm, SKC Inc.) filters were equilibrated for a minimum of 24 h under specific temperature (26 °C ± 2) and humidity (50% ± 2) conditions before and after sampling in a weighing room. All samples were weighed before and after sampling using a microbalance (XP26, Mettler-Toledo, Columbus, OH, USA). Prior to air sampling, the FTIR background of each PVC and MCE filter was measured and saved. The particle suspension method was the same as described above. Particles larger than the respirable-size

Table 1
Asbestos and their nonasbestiform analogues.

Asbestos			Nonasbestiform analogues		
Type	Source	Reference	Type	Source	Reference
Actinolite	NIST[a]	NIST SRM[b] 1867	Actinolite	near Wrightwood, San Bernadino Co., CA	[13]
Amosite	NIST[a]	NIST SRM[b] 1866	Grunerite	Marquette Co., MI	[47]
Anthophyllite	Palm Springs, CA	RTI[c] internal report	Anthophyllite	Kopparberg, Sweden	[13]
Chrysotile	NIST[a]	NIST SRM[b] 1866	Antigorite	Estrie, Quebec, Canada	Not available
Crocidolite	NIST[a]	NIST SRM[b] 1866	Riebeckite	Pike's Peak, Colorado Springs, CO	[19]
Tremolite	Lone Pine, CA	[14,19]	Tremolite	NIEHS[d]	[13,19]

[a] National Institute of Standards and Technology
[b] Standard Reference Material
[c] Research Triangle Institute International
[d] National Institute of Environmental Health Sciences

fraction were removed using a Higgins-Dewell cyclone (HD cyclone, 2.2 liter/min), and the respirable-size fraction was collected on the filter attached to a cowl sampling head (Part number: 225–3-23, SKC Inc.) (Fig. 1). After sampling, the FTIR spectrum of each sample was obtained using the portable FTIR (described above) and the saved file of the filter as a background.

2.4. Multivariate data analysis

This study utilized the PLS_Toolbox (v8.9.1) and undertook multivariate data analysis involving principal component analysis (PCA) and partial least squares-discriminant analysis (PLS-DA) to elucidate patterns of similarity within FTIR spectra derived from six distinct mineral types. The comprehensive spectral range (400–1200 wavenumbers) of each sample was employed in all subsequent data analyses. PCA and PLS-DA serve different purposes in multivariate data analysis. Both types of models use the shape of the FTIR spectra as a basis for analysis, and seek to group the spectra based on relative similarity to all other spectra in the training data. The closer the spectral profile of a sample is to another sample, the closer the two samples will appear on a score plot, while dissimilar spectra will cluster further apart. Using this concept as a base, PCA is primarily used for data reduction and visualization. It identifies the orthogonal (uncorrelated) components (principal components) that explain the maximum variance in the data. PCA doesn't consider class labels or groupings; it focuses solely on variance.

PLS-DA, on the other hand, is specifically designed for classification and discrimination tasks. It seeks to find the components (latent variables) that maximize the separation between predefined groups or classes in the data. In the PLS-DA models, there is a class (mineral) for each sample and all samples must belong to one of the predefined classes. When cross-validating the PLS-DA model, the algorithm will leave out the class data from a subset of the data, then try and predict the class and use the known class information to see if it correctly predicted the class or not. The partial least squares (PLS) algorithm was first introduced for regression tasks and then evolved into a classification method that is well known as PLS-DA [23] and has been used in a variety of applications [5]. The specific application of the PLS-DA algorithm to classify unknown minerals as asbestiform or nonasbestiform has not been done.

2.4.1. Principal component analysis (PCA)

For PCA analysis, the data was preprocessed via Savitzky–Golay 1st derivative (second order polynomial with a 15-wavenumber smoothing window), 1-normalization, followed by mean centering. When analyzing the KBr data, the suggested first seven principal components (PCs) were used, accounting for 97.90% of the total variance in the data, with 56.23% occupied by the first two PCs. When analyzing the PVC data, the first six PCs were used, accounting for 79.77% of the total variance in the data, with 43.72% occupied by the first two PCs. Both PCA models were cross-validated using Venetian blinds with 10 splits and a blind thickness of 1 with a resulting root mean square error of cross-validation (RMSECV) of 0.0006 for the KBr data and 0.0007 for the PVC model.

2.4.2. Partial least squares-discriminate analysis (PLS-DA)

For PLS-DA analysis, the data was preprocessed via Savitzky–Golay 1st derivative (second order polynomial with a 15-wavenumber smoothing window), 1-normalization, followed by mean centering before hierarchical cluster analysis via Ward's method and PLS-DA. When analyzing the KBr data, the first seven latent variables (LVs) were used to best represent the data. The seven LVs account for 96.878% of the variance with the first two LVs accounting for 55.41% of the total variance in the data. When analyzing the PVC data, the first six LVs were used, accounting for 79.72% of the total variance in the data with 43.58% being occupied by the first two LVs. Both PLS-DA models were cross-validated using Venetian blinds with 10 splits and a blind thickness of 1 with a cross-validation class error average of 0.06 for the KBr data and 0.007 for the PVC model. Class error is defined as the average of false positive rate and false negative rate for each class (1 – (sensitivity + specificity)/2).

2.4.3. Challenge sample preparation

To evaluate the PLS-DA models, 12 different challenge KBr pellet samples (3 KBr pellet samples of single asbestos (sample #1-#3), 3 KBr pellet samples of single nonasbestiform minerals (sample #4-#6), and a 6-KBr pellet mixture of each asbestos type and its nonasbestiform analogue (sample #7-#12)) were prepared. After FTIR measurement, the spectra were processed with PLS-DA followed by a prediction plot. The composition of each sample was predicted, and the asbestos types were quantified in each challenge sample using predicted percent composition (%).

3. Results

A total of 84 KBr pellet samples (7 samples of each mineral) were prepared, and the masses of samples ranged from 0.02 mg to 0.515 mg. A total of 120 PVC filter samples (10 samples of each mineral) were prepared, and the masses of the samples ranged from 0.008 mg to 2.307 mg. Examples of FTIR spectra of six regulated asbestos types in KBr pellets and on PVC filters, along with each sample mass, are shown in Fig. 2. The air samples with MCE filters were initially prepared, but due to the presence of strong absorbance (>6 absorbance units) observed at 1650, 1634, 1294, 1057, 851, and 832 cm^{-1}, the MCE filters were dropped from the study.

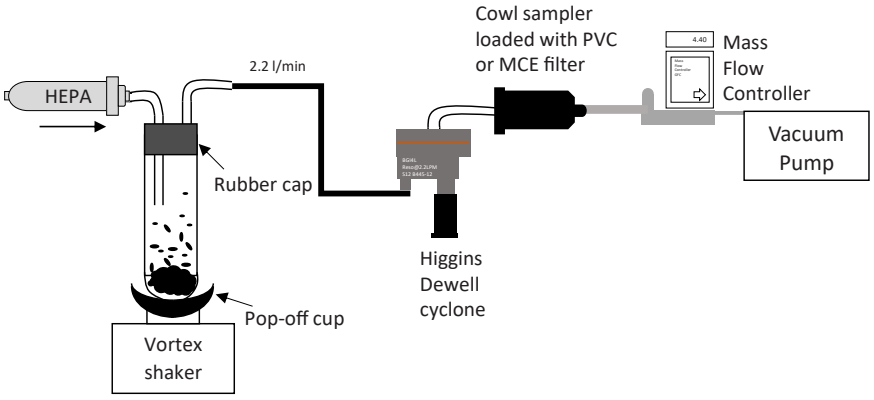

Fig. 1. Experimental setup for air sampling of respirable-size fraction.

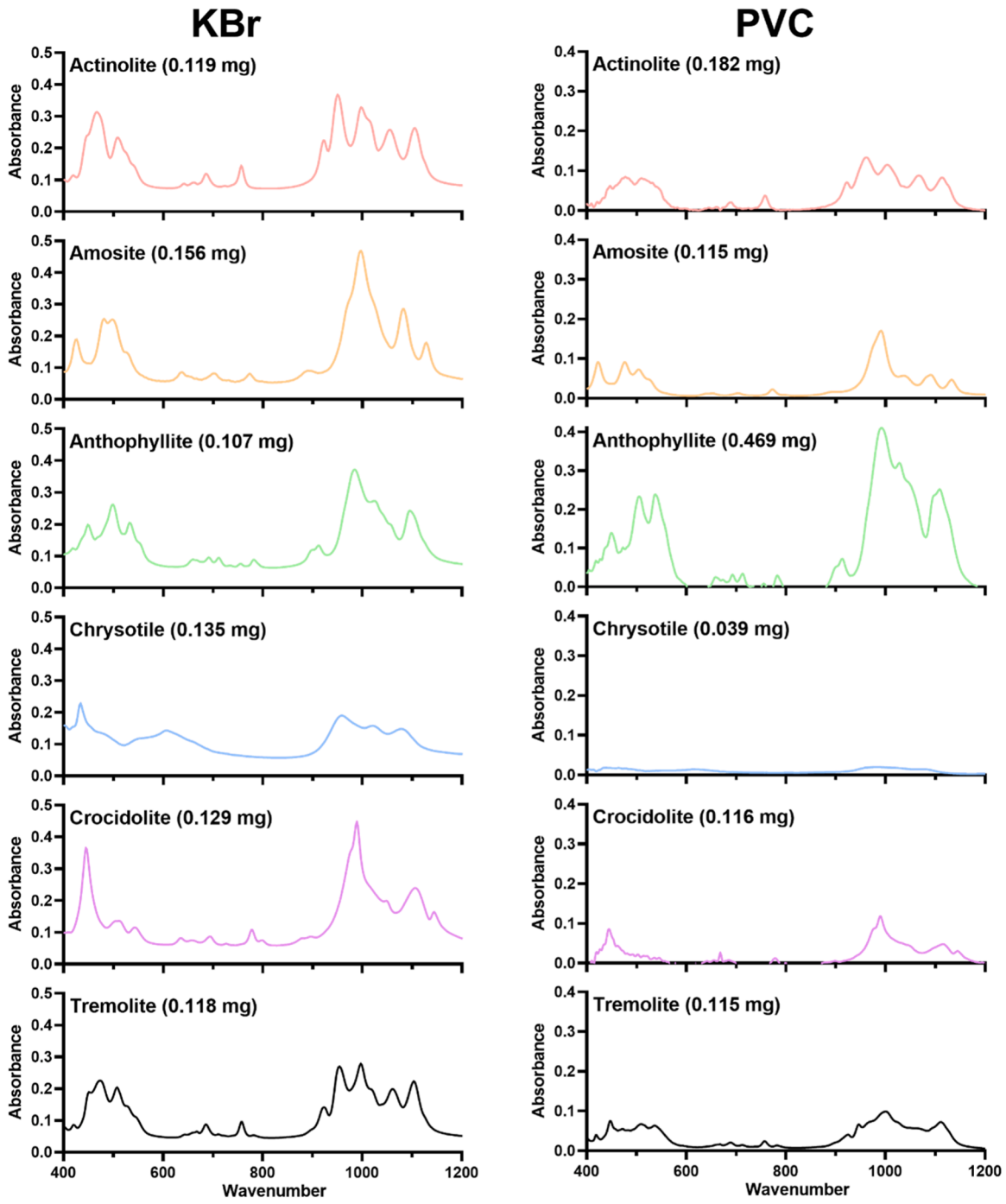

Fig. 2. FTIR spectra of six regulated asbestos types in the KBr pellets (top) and on PVC filters (bottom) with gravitational analysis results.

3.1. Principal component analysis (PCA)

In an attempt to discern if FTIR data can be used to differentiate between asbestos and their nonasbestiform analogues, PCA was used as a form of dimensionality reduction via hierarchical clustering, as shown in Fig. 3 for (top) KBr pellet samples and (bottom) PVC filter samples. On a PCA score plot, two samples having similar FTIR spectral profiles were located closer to each other and the furthest away from any samples that have the most different FTIR spectrum.

3.2. Partial least squares-discriminate analysis (PLS-DA)

As a secondary form of clustering analysis, PLS-DA was employed, and the first two LVs are shown in Fig. 4 (top) for KBr pellet samples and (bottom) for PVC filter samples. All of the clustering analyses show very distinct clustering of samples by mineral with chrysotile separating furthest from the five amphiboles. Additionally, within each mineral type, the asbestiform variant subclusters are apart from the non-asbestiform, which indicates that even within the same mineral type it is possible to assess the presence of EMPs and successfully classify a sample as asbestiform. Utilizing the relatively small sample set generated in this study, after cross-validation the PLS-DA analysis of KBr data had an average classification error of 0.007, indicating that there is a 0.7% chance of misclassifying a newly added sample. Similarly, the PVC data has an average classification error of 0.046. This translates to a 95% probability for a pure sample of unknown mineralogy collected on a PVC

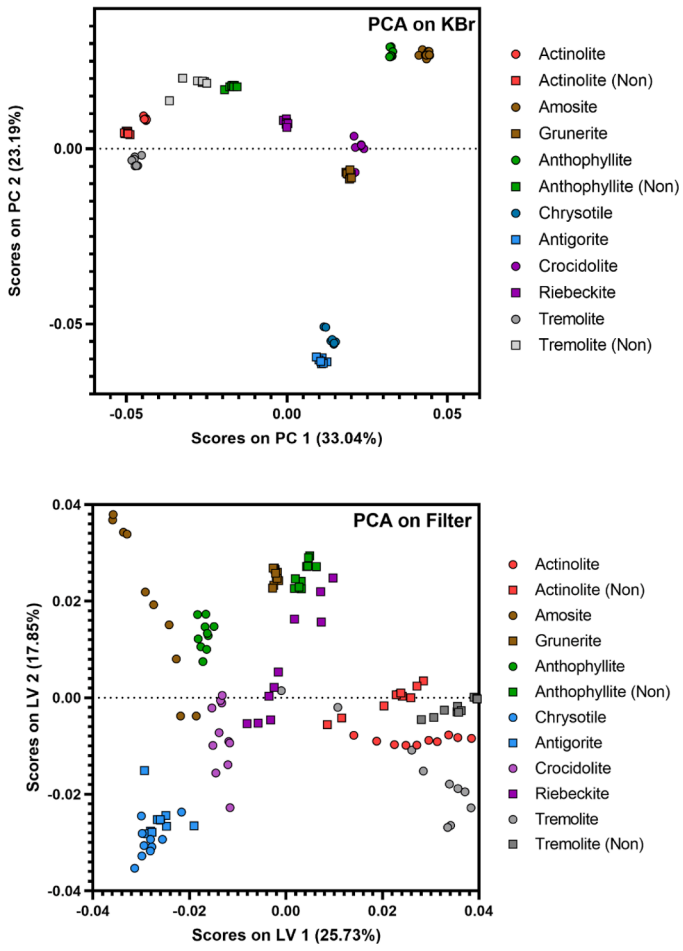

Fig. 3. Classification of asbestos and their analogues in a PCA score plot with KBr pellet samples (top) and air sample on PVC filters (bottom).

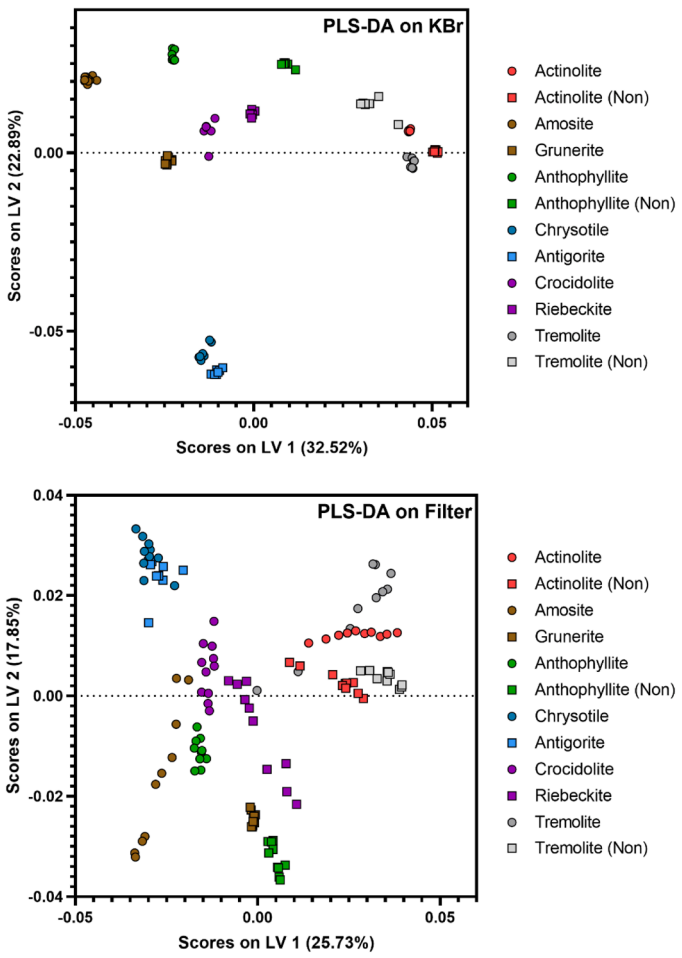

Fig. 4. Classification of asbestos and their analogues in a PLS-DA score plot with KBr pellet samples (top) and air sample on PVC filters (bottom).

filter to be correctly classified using FTIR spectra with the PLS-DA, given it is one of the 6 mineral types in the model. The use of the PVC filter instead of KBr pellets adds a layer of complexity to the analysis due to the presence of the filter (which is not exactly the same for each sample) and thus it is in general expected to predict slightly worse than the KBr.

3.3. *Prediction of challenge sample*

One benefit of running classification modeling is using the model to predict the composition of unknown samples. To accomplish this, 12 challenge samples with a known composition consisting of a single mineral or a mixture of each asbestos type and its nonasbestiform analogue were prepared and the model predicted the composition. The PLS-DA predicted composition of the asbestos types (%) is shown in Fig. 5 together with the actual mass content of each type of asbestos (%) for each mixed sample. Shown in each predicted donut plot are the two highest % composition minerals, and all other predicted minerals are grouped together into "other." As an example, the first challenge sample #1 was estimated to contain 100% amosite, and the model predicted the sample to be 91% amosite, 2% nonasbestiform actionolite, and 7% other minerals. The PLS-DA model would always predict the correct mineral of challenge samples, although the predicted composition (%) of samples #6 and #12 were lower than the actual one. For sample #6, the model failed to differentiate between the asbestiform and nonasbestiform habits of the same mineral. Sample #6 was 100% nonasbestiform tremolite while the prediction levels were 32% nonasbestiform tremolite, 20% tremolite, 11% actinolite, 5% nonasbestiform actinolite, 10% crocidolite, 10% anthophyllite and 12% other minerals. Sample #12 was 49% of tremolite and 51% of nonasbestiform tremolite, while the prediction levels were 25% of tremolite, 29% nonasbestiform tremolite, 14% actinolite, 11% nonasbestiform actinolite, 8% crocidolite, and 13% other minerals.

4. Discussion

The use of FTIR and PCA or PLS-DA for measurement of asbestos types and their nonasbestiform analogues could be applied for qualitative and/or quantitative bulk and/or airborne sample analysis; however, additional research is needed to fully develop this method.

4.1. *Multivariate data analysis*

Although the PLS-DA did not provide 100% correct mineral composition predictions for KBr pellet challenge samples, the prediction level can be improved with more data or through using a series of models. It should also be noted that these models were not trained on any mixed samples and only had access to the FTIR spectra of pure minerals, and the study was then asked to make predictions on mixed samples. Adding additional samples of pure minerals to the training data for the models will only strengthen the predictive models of future unknown mixed samples. Stach et al., [50,51] showed a near 1:1 relationship between gravitational mass and predicted mass of calcite, dolomite, and quartz in mixed mineral samples using FTIR and partial least square regression algorithm. Additionally, larger training datasets can enhance accuracy in all types of machine learning by reducing the chances of data overfitting in a larger sample size [4]. A recently

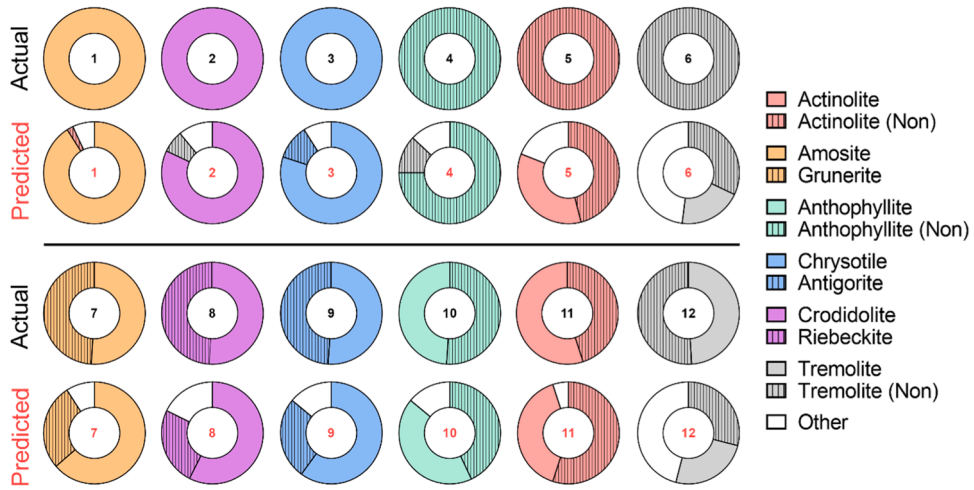

Fig. 5. Actual mass content (%) and PLS-DA predicted composition (%) of the asbestos and their nonasbestiform analogue types for each sample.

published article using a PLS model to predict silica from FTIR data found that the presence of known confounders reduced the silica prediction accuracy, but the effect was mitigated as the sample size of confounder data in the training data grew [55]. The prediction level of sample #5 was 35% actinolite and 46% nonasbestiform actinolite, while the actual sample was 100% nonasbestiform actinolite. This indicates that in the case of challenge sample #5, theoretically, the addition of more samples specifically of actinolite and nonasbestiform actinolite might improve its accuracy, although the number of the samples needed for a better prediction is still unknown. The prediction levels of sample #6 were 20% tremolite, 32% nonasbestiform tremolite, 16% actinolite, and nonasbestiform actinolite, while the actual sample was 100% nonasbestiform tremolite. The poor prediction level of the tremolite might be attributable to the similar spectral pattern between the actinolite and tremolite (Fig. 2), and their positions in the PLS-DA score plot (Fig. 4) were close to each other, again indicating the relative spectra. In addition, peak positions of actinolite and tremolite in the low wavenumber range region (<1200 cm^{-1}) were almost identical [52].

4.2. Method development

The NIOSH method 9002, Asbestos (bulk) by polarized light microscope (PLM), is described as "useful for the qualitative identification of asbestos and the semi-quantitative determination of asbestos content of bulk samples." This method has several limitations related with microscopic fiber analysis: "1) the method is not applicable to samples containing large amounts of fine fibers below the resolution of the light microscope, 2) other fibers with optical properties similar to the asbestos minerals may give positive interferences, 3) optical properties of asbestos may be obscured by coating on the fibers, 4) fibers finer than the resolving power of the microscope (ca. 0.3 μm) will not be detected and 5) heat and acid treatment may alter the index of refraction of asbestos and change its color [40]." The asbestos measurement with FTIR and multivariate data analysis might resolve these limitations, and the sample preparation process of the PLM analysis could be minimized. The identification of six regulated asbestos types in the asbestos-containing materials (ACM) with an updated PLS-DA model should be compared to the PLM analysis. Common minerals and materials of the ACM should be included in the calibration process.

In the current standard methods, the exposure levels of the RCS can be estimated from an absorbance at 800 cm^{-1} peak or area ([42], Method 7602, 7603; [36], P-7 Method), and a similar approach at a specific wavenumber can be applied for the quantification of the airborne asbestos exposure. It should be noted that the PLS-DA model is employing FTIR spectra between 1200–400 cm^{-1}, not an individual wavenumber, and the model may estimate exposure levels if the sample is within the calibration range [48,55]. A comparison would be necessary between the linear calibration method and PLS-DA for a better quantitative strategy. The current Occupational Exposure Levels (OELs) for asbestos is number based ([39], Method 7400, 0.1 asbestos fiber/cc), but the present study constructed mass-based calibration. A clear relationship between fiber number and mass should be addressed. Air sampling can be conducted for airborne fibers in a calm air chamber with an optimum filter loading (100–1300 fibers/mm^2) to ensure consistent counting [41]. The mass of fibers can be estimated using a gravitational analysis, and the number of fibers can be also estimated using the PCM fiber count in the sample. Although the mass might be dependent on the different asbestos types and size due to the difference on the specific gravity, the difference would be small. Alternatively, without addressing the relationship between mass and number of fibers, the PLS model can be trained to predict fiber count if the fiber concentration information is made available to the model.

Low detection limit (LOD) of both for bulk and air samples analysis should be evaluated. Gadsden et al. [12] prepared KBr pellet samples after ashing (450 °C for an hour) the air sampling filters and reported ~10 μg of LOD for airborne chrysotile at wave band 2.72 μm (3676 cm^{-1}) that is associated with the vibration of lattice of hydroxyl groups. Employing a smaller diameter of KBr pellet (1-mm pellet) can lower the detection limit by 10 ng [30]. An increased RCS FTIR absorbance unit in a smaller particle deposit area was reported [25]. A better classification accuracy was observed when the samples were prepared with KBr for both PCA and PLS-DA (Figs. 3 and 4). In addition, a larger absorbance unit (around more than 2 times higher) in the KBr pellets samples was found and compared to the samples on the PVC filter with similar mass (Fig. 2). Although extra sample preparation procedures including removing air sampling filters and making KBr pellets can be involved, the procedure can reduce uncertainties from direct-on-filter (DOF) FTIR measurement. The PVC filter for the air sampling can be ashed using low temperature or muffle furnace [42,43].

The FTIR spectra of the samples were only obtained through transmission-absorption analysis which might have had an uncertainty of the thickness of the pellet. Alternatively, diffuse reflectance IR spectroscopy (DRIFT) mode, where the IR beam is scattered by the sample surface, collected by the mirror, and sent to the detector, can be another method to be evaluated. The sample preparation step of the DRIFT is simply putting samples on the DRIFT sample holder; and it is a fast and non-destructive method [1,49,52], which could help to increase sample number in a short period of time. Asbestos quantification in asbestos-containing materials using the DRIFT technique showed promising results [1,49]. Near-infrared (NIR) spectrometer

measurement showed strong hydroxyl (O-H, 7300–7000 cm^{-1}) stretching vibration signals on the ACM [28,56], and an NIR (4000–10, 000 cm^{-1}) combination with PCA or PSL-DA might be another method to investigate.

Searching suitable air sampling filters for the airborne asbestos or other EMPs DOF analysis can be another area to investigate. Other commercially available membrane filters including polypropylene, polyethylene, silver membrane, nylon, and others can be evaluated [10].

The source (collected location) for the asbestos reference materials is always indicated in the samples, and it is still a question that there are FTIR spectra variations in the same asbestos type collected at a different source. The present study used the NIST SRM (actinolite, amosite, chrysotile, and crocidolite) and well-characterized amphibole materials (anthophyllite and tremolite); however, no such well-characterized nonasbestiform materials are available for research purposes.

The analysis method utilized in the current study can also be applied for analysis of nonregulated but hazardous EMPs such as Libby amphiboles, erionite, and taconite mine dust. In addition, this method may be especially useful in testing for the presence of asbestos and other potentially harmful amphibole particles in talc used in cosmetics and other consumer products that can affect cosmetic product safety. The Food and Drug Administration (FDA) is currently looking for improved methods to quantify the presence of EMPs in talc.

Finally, NIOSH developed the Field Analysis of Silica Tool (FAST, Version 1.0.8) software, and it is publicly available to process FTIR data of the RCS and to calculate exposure estimates. In the future, a similar software may be created for the qualification and quantification of the hazardous EMPs. The morphology and fiber-size analysis are not available with the method, and additional microscope analysis should be necessary.

5. Conclusions

This study is the first attempt at analyzing FTIR spectra using multivariate data analysis techniques for the classification of the asbestos types and their nonasbestiform analogues with bulk (KBr) and air samples (PVC). Classification of asbestos types with this method is possible, and classification of asbestos and their nonasbestiform analogues is also possible on PCA and PLS-DA score plots, limited by the fact that the study was conducted at controlled laboratory conditions with a small number of well-characterized reference samples. Improvements are needed for a better prediction in mixed samples, by adding known mixtures to the training data. The analysis of the FTIR spectra using PCA or PLS-DA for the EMP measurement may be applied for qualitative and/or quantitative bulk and/or airborne asbestos sample analysis. However, further research is needed to validate the procedures by comparing them to the current standard asbestos analytical methods and to develop the method(s) for the real samples that have an unknown origin and composition.

Environmental implication

The present study describes asbestos, a known carcinogen, and their nonasbestiform analogues classification using FTIR and multivariate data analysis. This novel method may resolve issues from other standard analysis methods. The phase contrast microscope (PCM) does not differentiate between asbestos and other fibers, polarized light microscope (PLM) is only for bulk asbestos materials and transmission electron microscope (TEM) is an expensive instrument, requiring extensive training and experienced microscopists. If the prediction from the multivariate data analysis is satisfactory as the study discussed, the method could estimate asbestos types and exposure concentrations, allowing for improved control of hazardous emissions.

Disclaimer

The findings and conclusions in this report are those of the authors and do not necessarily represent the official position of the National Institute for Occupational Safety and Health (NIOSH), Centers for Disease Control and Prevention (CDC). Mention of any company name or product does not constitute endorsement by NIOSH.

Funding

The National Institute for Occupational Safety and Health (NIOSH), Project #9390BMJ: Understanding elongate mineral particle exposure in mining.

CRediT authorship contribution statement

Cody Wolfe: Writing – review & editing, Visualization, Software, Formal analysis. **Taekhee Lee:** Writing – original draft, Visualization, Methodology, Investigation, Conceptualization. **Steven Mischler:** Writing – review & editing, Methodology, Investigation, Conceptualization.

Declaration of Competing Interest

The authors declare that they have no known competing financial interests or personal relationships that could have appeared to influence the work reported in this paper.

Data Availability

Data will be made available on request.

References

[1] Accardo, G., Cioffi, R., Colangelo, F., D'Angelo, R., De Stefano, L., Paglietti, F., 2014. Diffuse reflectance infrared fourier transform spectroscopy for the determination of asbestos species in bulk building materials. Materials 7 (1), 457–470. https://doi.org/10.3390/ma7010457.

[2] Barauna, V.G., Singh, M.N., Barbosa, L.L., Marcarini, W.D., Vassallo, P.F., Mill, J. G., et al., 2021. Ultrarapid on-site detection of SARS-CoV-2 infection using simple ATR-FTIR spectroscopy and an analysis algorithm: high sensitivity and specificity. Anal Chem 93 (5), 2950–2958. https://doi.org/10.1021/acs.analchem.0c04608.

[3] Beckett, S.T., Middleton, A.P., Dodgson, J., 1975. The use of infrared spectrophotometry for the estimation of small quantities of single varieties of U.I.C. C asbestos. Ann Occup Hyg 18 (4), 313–320. https://doi.org/10.1093/annhyg/18.4.313.

[4] Belay, T.K., Dagnachew, B.S., Boison, S.A., Ådnøy, T., 2018. Prediction accuracy of direct and indirect approaches, and their relationships with prediction ability of calibration models. J Dairy Sci 101 (7), 6174–6189. https://doi.org/10.3168/jds.2017-13322.

[5] Brereton, R.G., 2009. Chemometrics for Pattern Recognition. John Wiley & Sons Ltd, Chichester, England.

[6] Cauda, E., Chubb, L., Miller, A., 2016. Silica adds to respirable dust concerns: what if you could know the silica dust levels in a coal mine after every shift? Coal Age 121 (1), 31–33.

[7] Cauda, E., Chubb, L., Reed, R., Stepp, R., 2018. Evaluating the use of a field-based silica monitoring approach with dust from copper mines. J Occup Environ Hyg 15, 732–742.

[8] Ramazzini, Collegium, 2010. Asbestos is still with us: repeat call for a universal ban. Arch Environ Occup Health 65 (3), 121–126. https://doi.org/10.1080/19338241003776104.

[9] Dodson, R.F., Hammar, S.P., 2006. Asbestos: Risk Assessment. Epidemiology, and Health Effects, 1st ed.,. Boca Raton, FL: Taylor & Francis Group.

[10] Farcas, D., Lee, T., Chisholm, W.P., Soo, J.C., Harper, M., 2016. Replacement of filters for respirable quartz measurement in coal mine dust by infrared spectroscopy. J Occup Environ Hyg 13 (2), D16–D22. https://doi.org/10.1080/15459624.2015.1091962.

[11] Furuya, S., Chimed-Ochir, O., Takahashi, K., David, A., Takala, J., 2018. Global asbestos disaster. Int J Environ Res Public Health 15, 1000. https://doi.org/10.3390/ijerph15051000.

[12] Gadsden, J.A., Parker, J., Smith, W.L., 1970. Determination of chrysotile in airborne asbestos by an infra-red spectrometric technique. Atmos Environ 4 (6), 667–670.

[13] Harper, M., Lee, E.G., Doorn, S.S., Hammond, O., 2008. Differentiating non-asbestiform amphibole and amphibole asbestos by size characteristics. J Occup Environ Hyg 5 (12), 761–770.

[14] Harper, M., Gosen, Van, Crankshaw, B., Doorn, O.S., Ennis, S.S., Harrison, S. E, T. J., 2015. Characterization of lone pine, California, tremolite asbestos and preparation of research material. Ann Occup Hyg 59 (1), 91–103.
[15] Ham, S.H., Hwang, S.H., Yoon, C., Park, D., 2009. Review on asbestos analysis. J Korean Soc Occup Environ Hyg 19 (3), 213–232.
[16] Hart, J.F., Autenrieth, D.A., Cauda, E., Chubb, L., Spear, T.M., Wock, S., et al., 2018. A comparison of respirable crystalline silica concentration measurements using a direct-on-filter Fourier transform infrared (FT-IR) transmission method vs. a traditional laboratory X-ray diffraction method. J Occup Environ Hyg 15, 743–754. https://doi.org/10.1080/15459624.2018.1495334.
[17] IARC, 2012. A Review of Human Carcinogens. Part C: Arsenic. Metals, Dusts, and Fibres. International Agency for Research on Cancer.
[18] IARC, 2017. IARC Working Group on the Evaluation of Carcinogenic Risks to Humans. Some Nanomaterials and Some Fibres. International Agency for Research on Cancer.
[19] Khaliullin, T.O., Kisin, E.R., Guppi, S., Yanamala, N., Zhernovkov, V., Shvedova, A. A., 2020. Differential responses of murine alveolar macrophages to elongate mineral particles of asbestiform and non-asbestiform varieties: cytotoxicity, cytokine secretion and transcriptional changes. Toxicol Appl Pharmacol 409. https://doi.org/10.1016/j.taap.2020.115302.
[20] Kimmerle, F.M., Noel, L., Khorami, J., 1984. Quantitative IR-ATR spectrometry of asbestos fibers on membrane filters. Can J Chem 62, 441–451.
[21] Ku, B.K., Deye, G., Turkevich, L.A., 2013. Characterization of a vortex shaking method for aerosolizing fibers. Aerosol Sci Technol 47 (*12*), 1293–1301.
[22] Ku, B.K., Deye, G., Turkevich, L.A., 2017. Screen collection efficiency of airborne fibers with monodisperse length. J Aerosol Sci 115, 250–262.
[23] Lee, L.C., Liong, C.Y., Jemain, A.A., 2018. Partial least squares-discriminant analysis (PLS-DA) for classification of high-dimensional (HD) data: a review of contemporary practice strategies and knowledge gaps. Analyst 143 (15), 3526–3539.
[24] Lee, T., Ku, B.K., Walker, R., Kulkarni, P., Barone, T., Mischler, S., 2020. Aerodynamic size separation of glass fiber aerosols. J Occup Environ Hyg 17 (6), 301–311. https://doi.org/10.1080/15459624.2020.1742915.
[25] Lee, T., Lee, L., Cauda, E., Hummer, J., Harper, M., 2017. Respirable size-selective sampler for end-of-shift quartz measurement: development and performance. J Occup Environ Hyg 14 (5), 335–342. https://doi.org/10.1080/15459624.2016.1252845.
[26] Lee, T., Thorpe, A., Cauda, E., Tipton, L., Sanderson, W.T., Echt, A., 2018. Laboratory comparison of new high flow rate respirable size-selective sampler. J Occup Environ Hyg 15 (10), 755–765. https://doi.org/10.1080/15459624.2018.1503670.
[27] Lemen, R.A., Landrigan, P.J., 2017. Toward an Asbestos Ban in the United States. Int J Environ Res Public Health 14 (11), 1302.
[28] Lewis, I.R., Chaffin, N.C., Gunter, M.E., Griffiths, P.R., 1996. Vibrational spectroscopic studies of asbestos and comparison of suitability for remote analysis. Spectrochim Acta Part A 52, 315–328.
[29] Lippmann, M., 2014. Toxicological and epidemiological studies on effects of airborne fibers: coherence and public [corrected] health implications. Crit Rev Toxicol 44 (8), 643–695.
[30] Luoma, G.A., Yee, L.K., Rowland, R., 1982. Determination of microgram amounts of asbestos in mixtures by infrared spectrometry. Anal Chem 54 (12), 2140–2142.
[31] Manning, C.B., Vallyathan, V., Mossman, B.T., 2002. Diseases caused by asbestos: mechanisms of injury and disease development. Int Immunopharmacol 2, 191–200.
[32] Medeghini, L., Mignardi, S., De Vito, C., Conte, A.M., 2016. Evaluation of a FTIR data pretreatment method for principal component analysis applied to archaeological ceramics. Microchem J 125, 224–229.
[33] Miller, A.L., Drake, P.L., Murphy, N.C., Noll, J.D., Volkwein, J.C., 2012. Evaluating portable infrared spectrometers for measuring the silica content of coal dust. J Environ Monit 14, 48–55.
[34] Miller, A.L., Drake, P.L., Murphy, N.C., Cauda, E.G., LeBouf, R.F., Markevicius, G., 2013. Deposition uniformity of coal dust on filters and its effect on the accuracy of FTIR analyses for silica. Aerosol Sci Technol 47, 724–733.
[35] Miller, A.L., Weakley, A.T., Griffiths, P.R., Cauda, E.G., Bayman, S., 2017. Direct-on-filter α-quartz estimation in respirable coal mine dust using transmission fourier transform infrared spectrometry and partial least squares regression. Appl Spectrosc 71, 1014–1024.
[36] Mine Safety and Health Administration (MSHA). 2013. Pittsburgh Safety and Health Technology Center: Infrared determination of quartz in respirable coal mine dust: Method P-7. Pittsburgh, PA: U.S. Department of Labor.
[37] Morais, C.L.M., Lima, K.M.G., Singh, M., Martin, F.L., 2020. Tutorial: multivariate classification for vibrational spectroscopy in biological samples. Nat Protoc 15, 2143–2162. https://doi.org/10.1038/s41596-020-0322-8.
[38] Müller, C.M., Pejcic, B., Esteban, L., Piane, C.D., Raven, M., Mizaikoff, B., 2014. Infrared attenuated total reflectance spectroscopy: an innovative strategy for analyzing mineral components in energy relevant systems. Sci Rep 4 (1), 6764.
[39] National Institute for Occupational Safety and Health (NIOSH): Asbestos and other fibers by PCM, (NIOSH7400, NIOSH Manual of Analytical Methods 5th ed.). Cincinnati, OH: NIOSH, 2019.
[40] National Institute for Occupational Safety and Health (NIOSH): Asbestos (bulk) by PLM (NIOSH 9002, NIOSH Manual of Analytical Methods 4th ed.). Cincinnati, OH: NIOSH, 1994.
[41] National Institute for Occupational Safety and Health (NIOSH): NIOSH Manual of Analytical Methods 5th ed. Chapter FI Measurement of fibers, Cincinnati, OH: NIOSH, 2016.
[42] National Institute for Occupational Safety and Health (NIOSH): QUARTZ in coal mine dust, by IR (NIOSH7603, NIOSH Manual of Analytical Methods 5th ed.). Cincinnati, OH: NIOSH, 2017.
[43] National Institute for Occupational Safety and Health (NIOSH): Silica, Respirable crystalline, by IR (KBr pellet) (NIOSH7602, NIOSH Manual of Analytical Methods 5th ed.). Cincinnati, OH: NIOSH, 2017.
[44] National Institute for Occupational Safety and Health (NIOSH): Work-Related Lung Disease Surveillance System, Welcome to eWoRLD (cdc.gov), accessed on September 1, 2023.
[45] Navas, N., Romero-Pastor, J., Manzano, E., Cardell, C., 2008. Benefits of applying combined diffuse reflectance FTIR spectroscopy and principal component analysis for the study of blue tempera historical painting. Anal Chim Acta 630 (2), 141–149.
[46] Patterson, J.H., O'Connor, D.J., 1966. Chemical studies of amphibole asbestos. I. Structural changes of heat-treated crocidolite, amosite, and tremolite from infrared absorption studies. Aust J Chem 19 (7), 1155–1164.
[47] Characterization of Dadeville, AL, and Palm Springs, CA, anthophyllite asbestos, Summary Report, RTI project No. 0212288.004, 2012.
[48] Salehi, M., Zare, A., Taheri, A., 2021. Artificial neural networks (ANNs) and partial least squares (PLS) regression in the quantitative analysis of respirable crystalline silica by fourier-transform infrared spectroscopy (FTIR). Ann Work Expo Health 65, 346–357.
[49] Scardina, P., 2013. Agilent Technologies Quantitative determination of common types of asbestos by diffuse reflectance FTIR.
[50] Stach, R., Barone, T., Cauda, E., Krebs, P., Pejcic, B., Daboss, S., et al., 2020. Direct infrared spectroscopy for the size-independent identification and quantification of respirable particles relative mass in mine dusts. Anal Bioanal Chem 412, 3499–3508.
[51] Stach, R., Barone, T., Cauda, E., Mizaikoff, B., 2021. A novel calibration method for the quantification of respirable particles in mining scenarios using fourier transform infrared spectroscopy. Appl Spectrosc 75 (3), 307–316.
[52] Ventura, D.G., Vigliaturo, R., Gieré, R., Pollastri, S., Gualtieri, A.F., Iezzi, G., 2018. Infra red spectroscopy of the regulated asbestos amphiboles. Minerals 8, 413. https://doi.org/10.3390/min8090413.
[53] Wang, L., Mizaikoff, B., 2008. Application of multivariate data-analysis techniques to biomedical diagnostics based on mid-infrared spectroscopy. Anal Bioanal Chem 391, 1641–1654. https://doi.org/10.1007/s00216-008-1989-9.
[54] Weakley, A.T., Miller, A.L., Griffiths, P.R., Bayman, S.J., 2014. Quantifying silica in filter-deposited mine dusts using infrared spectra and partial least squares regression. Anal Bioanal Chem 406, 4715–4724.
[55] Wolfe, C., Lauren, C., Walker, R., Yekich, M., Cauda, E., 2022. Monitoring worker exposure to respirable crystalline silica: application for data-driven predictive modeling for end-of-shift exposure assessment. Ann Work Expo Health 66 (8), 1010–1021.
[56] Zholobenko, V., Rutten, F., Zholobenko, A., Holmes, A., 2021. In situ spectroscopic identification of the six types of asbestos. J Hazard Mater 403, 123951.